

348

5312-1N

ds SB 238520

June 2, 1986

Annual Report for Grant No. NAGW-319
Covering the Period from 15 May 1985 to 14 May 1986

PHOTOABSORPTION AND PHOTODISSOCIATION OF MOLECULES IMPORTANT
IN THE INTERSTELLAR MEDIUM

Submitted by:

Long C. Lee
Department of Electrical & Computer Engineering
San Diego State University
San Diego, CA 92182

Prepared for:

NASA Headquarters
Washington, D.C. 20546
Attention: Dr. Nancy W. Boggess
Astronomy/Relativity Branch
Code EZ

(NASA-CR-176828) PHOTOABSORPTION AND
PHOTODISSOCIATION OF MOLECULES IMPORTANT IN
THE INTERSTELLAR MEDIUM Annual Report, 15
May 1985 - 14 May 1986 (San Diego State
Univ., Calif.) 34 p HC A03/MF A01. CSCL 03B G3/90

N86-27171

Unclas
43079

TABLE OF CONTENTS

I.	Introduction.....	3
II.	Research Accomplished.....	3
	A. Photoabsorption Cross Section of SO.....	3
	B. Photoabsorption and Photodissociation of HCl.....	4
	C. Photoabsorption and Photodissociation of CH ₃ CN.....	4
	D. Photoabsorption and Photodissociation of H ₂ CO.....	5
	E. Windowless Apparatus.....	6
III.	Publications and Presentations Resulted in This Reporting Period.....	7
IV.	Appendices	
	A. "Vacuum Ultraviolet Photoabsorption Study of SO"	
	B. "Quantitative Photoabsorption and Fluorescence Study of HCl in Vacuum Ultraviolet"	
	C. "Photoabsorption Cross Section of CH ₃ CN: Photodissociation Rates by Solar Flux and Interstellar Radiation"	
	D. "Fluorescence from VUV Excitation of Formaldehyde"	

I. INTRODUCTION

In the period from May 15, 1985 to May 14, 1986, the photoabsorption and photodissociation cross sections of the interstellar radical of SO and the interstellar molecules of HCl, H₂CO, and CH₃CN were measured and the results were reported in scientific papers. In the meantime, we have constructed a windowless apparatus to be used for measuring the photoabsorption and photodissociation cross sections of CO in the 90-105 nm region. The optical data obtained in this research program are needed for the determination of the formation and destruction rates of molecules and radicals in the interstellar medium. Our accomplishments in this research period are summarized below.

II. RESEARCH ACCOMPLISHED

A. Photoabsorption Cross Section of SO

The photoabsorption cross section of SO was measured in the 115-200 nm region. The SO radicals were produced from a pulsed-discharge of a trace of SO₂ in a few torr of Ar. This technique has been used to measure the photoabsorption cross sections of OH, OD, and CN in previous periods. An absorption band of SO was observed in the 115-135 nm region with a peak cross section of $1.7 \times 10^{-16} \text{ cm}^2$ at 126 nm. The absorption cross section in the 135-200 nm region is quite small which was below our detection limit of $3 \times 10^{-18} \text{ cm}^2$.

The absorption cross section is a smooth function of excitation wavelength, indicating that the absorption is mainly a dissociative process. This result implies that the photo-

dissociation cross section is nearly equal to the photoabsorption cross section measured. The current data will be used to determine the photodissociation rate of SO by the interstellar radiation field. The experimental result has been summarized in a paper entitled "Vacuum Ultraviolet Photoabsorption Study of SO" which has been published in the Journal of Chemical Physics. The paper is attached in this report as Appendix A.

B. Photoabsorption and Photodissociation of HCl

The photoabsorption and fluorescence cross sections of HCl had been measured in the previous funding period. However, in the previous data analysis, we found that some of the absorption bands have very high absorption cross sections such that their absorbances were saturated by the pressures used in the measurement. The absorption cross section was remeasured in this funding period using very low gas pressure (less than 2 mtorr). The data have been analyzed completely in this period and the results were summarized in a paper to be published in the Journal of Chemical Physics. The paper is attached as Appendix B in this report.

C. Photoabsorption and Photodissociation of CH₃CN

The photoabsorption and fluorescence cross sections of CH₃CN have been measured in the 106-180 nm region using synchrotron radiation as a light source. Fluorescence from the photofragment of CN (A, B-X) in the ultraviolet-visible region was observed, and the fluorescence quantum yield was measured. The absorption spectrum shows discrete structure, but the quantum yield is a

smooth function of excitation wavelength, indicating that the photoexcitation of CH₃CN in the vacuum ultraviolet is mainly predissociative. The photodissociation cross section is thus nearly equal to the photoabsorption cross section. The photodissociation rate of CH₃CN by the interstellar radiation field in the 105-200 nm region is $2.2 \times 10^{-9} \text{ s}^{-1}$ as calculated from the photoabsorption cross section measured.

The result for CH₃CN has been summarized in a paper entitled "Photoabsorption Cross Section of CH₃CN: Photodissociation Rates by Solar Flux and Interstellar Radiation", which has been published in the Journal of Geophysical Research. The paper is attached as Appendix C in this report.

D. Photoabsorption and Photodissociation of H₂CO

The photoabsorption and fluorescence cross sections of H₂CO were measured in the 105-180 nm region using synchrotron radiation as a light source. Vacuum ultraviolet (VUV) emission from excited photofragments was dispersed and identified to be the CO(A¹Π → X¹Σ⁺) system. The vibrational population of CO(A) was determined from the fluorescence spectrum and was used to study the photodissociation mechanism. The threshold for the production of the VUV emission is at 140.3 nm. The UV emission from HCO* was observed at the threshold of 147.5 nm. The upper limit of the dissociation energy, D₀(H-HCO), determined from the HCO emission threshold is 3.61 eV. The quantum yield for the production of either CO* or HCO* is a smooth function of the excitation wavelength, from which two dissociative states with

vertical energies at 8.69 and 10.7 eV are derived. The VUV and UV fluorescences have maximum quantum yields at 116 nm of about 1.6% and 0.23%, respectively.

The result has been summarized in a paper entitled "Fluorescence from VUV Excitation of Formaldehyde", which has been accepted for publication in the Journal of Chemical Physics. A preprint is attached as Appendix D in this report.

E. Windowless Apparatus

A one-meter vacuum monochromator (McPherson Model 225) has been set-up in our laboratory, which is now being used to study the photodissociation and photoionization processes of interstellar molecules in the 50-105 nm region. The fluorescence from excited photofragment is dispersed by a 0.3-meter monochromator (McPherson Model 218). The emission species will be identified from the fluorescence spectra.

In the meantime, we are preparing a windowless apparatus in the Synchrotron Radiation Center at the University of Wisconsin. This apparatus will be used to measure the photoabsorption and photodissociation cross sections of interstellar molecules in the 90-105 nm region. We will use this apparatus to measure the photoabsorption and photodissociation cross section of CO in the next funding period.

III. Publications and Presentations Resulted in This Reporting Period

1. J. B. Nee and L. C. Lee, "Photodissociation Rates of OH, OD and CN by the Interstellar Radiation Field", *Astrophys. J.*, 291, 202 (1985).
2. J. B. Nee, M. Suto and L. C. Lee, "Photodissociation Processes of Hydrogen Halides Studied with Synchrotron Radiation", presented at the XIV International Conference on the Physics of Electronic and Atomic Collisions, Palo Alto, CA, July 24-30, 1985.
3. J. B. Nee and L. C. Lee, "Photoabsorption Cross Sections of Interstellar Free Radicals in the Vacuum Ultraviolet Wavelengths" presented at the 17th International Symposium on Free Radicals, Granby, CO, August 18-23, 1985.
4. M. Suto and L. C. Lee, "Photoexcitation Process of Cl₂ in VUV", presented at the 1985 SRC Users Group Meeting, Madison, Wis., October 21-22, 1985.
5. J. B. Nee, M. Suto and L. C. Lee, "Photoexcitation Processes of CH₃OH: Rydberg States and Photofragment Fluorescence", *Chem. Phys.* 98, 147 (1985).
6. M. Suto and L. C. Lee "Photoabsorption Cross Section of CH₃CN: Photodissociation Rates by the Solar Flux and the Interstellar Radiation Field", *J. Geophys. Res.*, 90, 13037 (1985).
7. J. B. Nee and L. C. Lee "Vacuum Ultraviolet Photoabsorption Study of SO", *J. Chem. Phys.*, 84, 5303 (1986).
8. J. B. Nee, M. Suto and L. C. Lee, "Quantitative Photoabsorption and Fluorescence Study of HCl in Vacuum Ultraviolet" *J. Chem. Phys.*, in press.
9. M. Suto, X. Wang, and L. C. Lee, "Fluorescence from VUV Excitation of Formaldehyde", *J. Chem. Phys.*, in press.

Appendix D

"Fluorescence from VUV Excitation of Formaldehyde"

Fluorescence from VUV Excitation of Formaldehyde

Masako Suto, Xiuyan Wang, and L. C. Lee
Department of Electrical & Computer Engineering
San Diego State University
San Diego, CA 92182

ABSTRACT

The photoabsorption and fluorescence cross sections of H_2CO were measured in the 105-180 nm region using synchrotron radiation as a light source. Vacuum ultraviolet (VUV) emission from excited photofragments was dispersed and identified to be the $\text{CO}(A^1\Pi \rightarrow X^1\Sigma^+)$ system. The vibrational population of $\text{CO}(A)$ was determined from the fluorescence spectrum and was used to study the photodissociation mechanism. The threshold for the production of the VUV emission is at 140.3 nm. UV emission from HCO^* was observed below a threshold of 147.5 nm. The upper limit of the dissociation energy, $D_0(\text{H-HCO})$, determined from the HCO emission threshold is 3.61 eV. The quantum yield for the production of either CO^* or HCO^* is a smooth function of the excitation wavelength, from which two dissociative states with vertical energies at 8.69 and 10.7 eV are derived. The VUV and UV fluorescences have maximum quantum yields at 116 nm of about 1.6% and 0.23%, respectively. The photodissociation process of H_2CO in VUV is discussed.

I. INTRODUCTION

Formaldehyde is one of the polyatomic organic molecules observed in the interstellar medium.¹ Quantitative data for the photodissociation processes of H₂CO are needed for the modeling of the H₂CO photochemistry in the interstellar medium. Also, H₂CO is a product of the reactions between O₃ and olefins, and its photodissociation data are needed for the study of atmospheric chemistry and combustion process. Because of such needs, this simplest aldehyde has attracted great attention in many fields. Earlier works have been summarized by Moule and Walsh.²

The VUV absorption spectrum of H₂CO has been extensively studied both experimentally³⁻⁷ and theoretically⁸⁻¹⁰. The discrete bands appeared in the 115-180 nm region are well analysed and are mostly attributed to Rydberg states.³⁻¹⁰ The absorption cross section of H₂CO has been measured^{5,6} in the 60-180 nm region. The result of Mentall and Gentieu⁵ in the 154-177 nm region was different from the earlier measurement of Fleming et al.⁴ This discrepancy has been corrected by the later measurement of Mentall et al.⁶, which is confirmed in the current measurement. The weak absorption cross section of H₂CO in the UV region was measured by McQuigg and Calvert¹¹.

The photodissociation process of H₂CO in the 180-300 nm region has been extensively studied.^{2,11,12} The possible primary photodissociation processes are,



The quantum yield for each process depends on the excitation wavelength. It was found that processes (1) and (2) are dominant in the UV region, because the sum of their quantum yields is about 1.

The photodissociation process of H_2CO in the VUV region is relatively less investigated and the results are controversial. Dyne and Style¹³ have observed fluorescence from the excited HCO^* by photodissociation of H_2CO with a H_2 discharge lamp. They suggested that the fluorescence was produced by excitation wavelengths shorter than 134.5 nm. However, Glicker and Stief¹⁴ could not detect the fluorescence using Kr (123.6 nm) and Xe (147.0 nm) resonance lamps. In the current experiment, the HCO^* fluorescence was observed at excitation wavelengths shorter than 147.5 nm. However, the cross section for the fluorescence was so small that it may not have been detected in the experiment of Glicker and Stief¹⁴. In addition, the CO(A-X) system in VUV region was observed in the current experiment. The fluorescence data are useful for the study of the photodissociation process of H_2CO in VUV.

In this experiment, the absorption and fluorescence cross sections of H_2CO were measured using synchrotron radiation as a light source. The oscillator strengths for discrete absorption bands were calculated from the measured absorption cross sections. The VUV fluorescence was dispersed to identify the emitting species, and the quantum yields for both the VUV and UV-visible fluorescence bands were measured.

II. EXPERIMENTAL

The experimental set-up for the synchrotron radiation measurement has been described in a previous paper.¹⁵ In brief, synchrotron radiation produced from the electron storage ring at the University of Wisconsin was dispersed by a 1-m vacuum monochromator. The dispersed photon beam entered the gas cell through a LiF window. The optical path length was 39.1 cm. The VUV light source was converted to the UV light by sodium salicylate coated outside the exit LiF window and then detected by a photomultiplier tube (PMT). The UV-visible fluorescence was monitored by a cooled PMT (EMI 9558QB) sensitive in the 180-800 nm region through a quartz window. The VUV fluorescence was observed through a LiF window by a solar blind PMT (EMI, CsI photocathode) sensitive in the 115 to 200 nm region. Dry N₂ gas was used to flush between the windows of the gas cell and the solar-blind PMT. The UV and VUV fluorescence bands were simultaneously observed in two directions perpendicular to the incident photon beam. The signals from the PMTs were processed by an ORTEC photon counting system, and then simultaneously recorded by a X-Y recorder and an IBM microcomputer.

For the experiment of fluorescence dispersion, H₂CO was irradiated by a NV line at 123.9 nm produced from a capillary-condensed-discharge light source (manufactured by the VUV Associates). The fluorescence in the VUV region was dispersed by a 1-m vacuum monochromator (McPherson 225) with a grating blazed at 120 nm and detected by a solar-blind PMT (Hamamatsu, R1459). The fluorescence in the UV-visible region was dispersed by a 0.3-

m monochromator (McPherson 218) and detected by a cooled PMT (EMI 9558QB). Both the VUV and UV-visible fluorescence bands were observed at a direction perpendicular to the light source.

Monomeric formaldehyde was obtained from vapor of solid paraformaldehyde in a stainless steel container which was warmed up to 50-80 °C. The freshly vaporized H₂CO monomer leaked into the gas cell through Teflon tubing and Teflon valves. The gas cell was continuously pumped by a sorption pump to maintain a constant pressure. This flow system minimized the contamination by impurities produced from photodissociation of H₂CO and outgassing of walls. The pressure in the gas cell was monitored by a MKS Baratron manometer.

III. RESULTS AND DISCUSSION

A. Absorption Cross Section

The absorption cross section was measured by the attenuation of photon flux by H₂CO at several pressures lower than 30 mtorr, where the absorbance, $\ln(I_0/I)$, depends linearly on the H₂CO pressure. The photoabsorption cross section in the 106-180 nm region measured with a spectral resolution of 0.2 nm is shown in Fig. 1a. (The low resolution was used in order to obtain sufficient light source intensity to measure the fluorescence cross section simultaneously). The experimental uncertainty is estimated to be within 10% of a given value.

As shown in Fig. 1a, the absorption spectrum at wavelengths longer than 115 nm is dominated by sharp discrete bands. The current result is consistent with the measurement of Mentall et al.⁶, which is somewhat different from their earlier data.⁵ For

a discrete band, the measured absorption cross section represents an average value over the monochromator bandwidth, so its value depends on the monochromator resolution. The lower resolution yields the lower peak cross section and the wider absorption bandwidth. The cross section at a sharp peak in Fig. 1a is about 20-30% lower than the values measured by Mentall et al.⁶, because their resolution (0.025-0.05 nm) is higher than the current one (0.2 nm).

In contrast to the absorption cross section, the oscillator strength does not depend on the resolution. The oscillator strength can be determined from the measured absorption cross sections as given by,¹⁶

$$f = 11.3 \int \sigma(\lambda) d\lambda / \lambda^2,$$

where $\sigma(\lambda)$ is the measured absorption cross section in units of Mb(10⁻¹⁸ cm²) and λ is the wavelength in unit of nm.

The oscillator strengths and the integrated absorption cross sections, $\int \sigma(\lambda) d\lambda$, for the strong absorption bands were calculated and listed in Table I. The oscillator strengths measured earlier by photoabsorption⁶ and electron scattering¹⁷ are also listed in Table I for comparison. The f values measured in this work agree well with the earlier values^{6, 17} measured with different experimental conditions and methods. These results demonstrate that as long as the photoabsorption cross section is measured at a low pressure (free from saturation problem), it can be used to calculate the oscillator strength.

The nature for the electronic transitions of absorption bands has been extensively studied.^{2, 6-10} The assignment of

Mentall et al.⁶ is indicated in Fig. 1a to identify the Rydberg states. The Rydberg states (ns, np and nd) converge to the first ionization potential at 114.2 nm.^{6,18,19} Two strong peaks at 135.1 and 137.2 nm were not assigned. According to Mentall et al.⁶, it may belong to the $1B_1$ valence state whose other vibrational levels distribute in the 136-145 nm region. The underlying continua in the 118-160 nm region indicates the existence of dissociative states.

B. Fluorescence Cross Section

Fluorescences from photoexcitation of H_2CO were observed in the VUV and UV-visible regions as shown in Figs. 1b and 1c. Dyne and Style¹³ have photographically dispersed the fluorescence from the excited photofragment of H_2CO using a H_2 arc discharge lamp as a light source. The fluorescence band in the 285.8-409.2 nm region was observed and attributed to the HCO "Hydrocarbon Flame" A band. This band was originally observed in hydrocarbon flame by Vaidya²⁰ and later identified as the $HCO(\tilde{B}^2A' \rightarrow \tilde{X}^2A')$ transition.²¹ In our experiment, optical filters were used to isolate the UV-visible fluorescence, and the fluorescence was found to be dominant at wavelengths shorter than 400 nm, indicating that the observed fluorescence is the same $HCO(\tilde{B}-\tilde{X})$ system. An attempt was made to disperse the UV fluorescence from photoexcitation of H_2CO at 123.9 nm in our experiment. Fluorescence in the 300-400 nm region was observed, but the intensity was too weak for the 0.3 m monochromator to resolve the vibrational structure with certainty.

The pressure dependence of the UV fluorescence intensity was investigated. The fluorescence intensity increases linearly with

pressure up to 20 mtorr. In this linear region, the fluorescence intensity at a fixed pressure was measured as a function of excitation wavelength. The fluorescence intensity was converted to the absolute fluorescence cross section by comparing its intensity with the OH(A-X) emission from photodissociation of H₂O, for which the absolute cross section is known.¹⁵ The absolute UV fluorescence cross section as a function of excitation wavelength is shown in Fig. 1c. Experimental uncertainty is estimated to be within 30% of a given value.

The HCO emission was not observed in the experiment of Glicker and Stief¹⁴ in contrast to the observation of Dyne and Style¹³. In this work, we confirm that the HCO emission does exist. However, the fluorescence quantum yield is so small (less than 0.23%) that the fluorescence may not have been detectable in the experiment of Glicker and Stief¹⁴. Therefore, the current quantitative result may bring a reconciliation for the previous controversy.

The emission in the VUV region is identified to be the CO fourth positive band (see next section for the dispersed spectrum). The resonance fluorescence of H₂CO itself is not expected to be significant because all excited states in the VUV region have a tendency to be predissociative (see more discussion in the quantum yield section). The absolute cross section for the production of the VUV fluorescence was calibrated by comparing the observed fluorescence intensity with the CO resonance fluorescence intensity. The CO resonance fluorescence cross section is assumed to be equal to the CO absorption cross

section measured with the same resolution. This assumption is justified below.

The CO fourth positive emission band spreads from VUV to UV. The intensity distribution was investigated in this experiment. The UV fluorescence cross section of CO was calibrated against the OH(A-X) emission from the H₂O photodissociation. It is found that the UV fluorescence cross section is less than 5% of total CO(A-X) fluorescence cross section. This ratio is consistent with the value estimated from the Franck-Condon factors²²⁻²⁴ and the electronic transition moment²⁵ of the CO(A-X) band. Thus, the assumption that the CO(A-X) resonance fluorescence cross section in the VUV region is equal to the absorption cross section is reasonably valid. The absolute VUV fluorescence cross section of H₂CO as a function of excitation wavelength is shown in Fig. 1b. The experimental uncertainty is estimated to be within 50% of a given value.

The VUV emission starts to appear around 140.3 nm, while the threshold of the UV emission is about 147.5 nm. The excitation spectra for both the VUV and UV fluorescences have structures very similar to the absorption spectrum. The cross sections for both fluorescences decrease significantly at wavelengths shorter than the first ionization limit at 114.2 nm. This may be due to photoionization being the dominant process at the short wavelength region.

C. Fluorescence Spectrum and Vibrational Population of CO*(A)

The fluorescence spectrum in the 140-175 nm region produced from photodissociative excitation of H₂CO at 123.9 nm (NV emission line) is shown in Fig. 2. The fluorescence spectrum is

identified as the $\text{CO}(A^1\Pi \rightarrow X^1\Sigma^+)$ system, whose wavelength positions are also indicated in Fig. 2 for comparison. The fluorescence mainly originates from the $v'=0-3$ vibrational levels. A $\text{CO}(A-X)$ emission spectrum (dispersed by the same monochromator with a resolution of 0.08 nm) produced from a microwave discharge of a trace of H_2CO in 0.5 torr of Ar was used to confirm this identification.

The CO fluorescence intensity increases linearly with the H_2CO pressure up to 100 mtorr. The fluorescence spectrum is independent on the gas pressure. This result is expected because the radiative lifetime (about 10^{-8} s²²) of $\text{CO}^*(A)$ is much shorter than the mean collisional time (about 10^{-6} s) of $\text{CO}^*(A)$ with other molecules in the gas cell.

The fluorescence spectrum can be used to determine the vibrational population. The fluorescence intensity is given by²²,

$$I_{v'v''} = K N_{v'} R_e^2 q_{v'v''} / \lambda_{v'v''}^3$$

where K is a constant including the geometrical factor and the detection efficiency, $N_{v'}$ is the population of the vibrational level v' , R_e is the electronic transition moment, $q_{v'v''}$ is the Franck-Condon factor, and $\lambda_{v'v''}$ is the emission wavelength.

The PMT response and the monochromator efficiency were almost constant (as specified by the manufacturers) in the studied fluorescence region. This constancy was checked by the $\text{CO}(A, v'=0 - X, v'')$ fluorescence spectrum. Combining this constant detection efficiency with the known Franck-Condon factors²²⁻²⁴ and the electronic transition moment,²⁵ the relative vibrational population of $\text{CO}^*(A)$ is determined as

$$N_0 : N_1 : N_2 : N_3 = 1 : 0.95 : 0.75 : 0.38$$

The excitation light source of 123.9 nm provides an excess energy of 1.92 eV over the $H_2+CO^*(A, v'=0)$ process whose threshold is 8.08 eV (see Section E). This excess energy could populate²² the $CO^*(A)$ species up to $v' = 11$ vibrational levels. However, the observed vibrational population is only in the lower levels, indicating that most of the excess energy may be converted into translational energy of the photofragments and/or taken away by H_2 as vibrational energy.

The vibrational population is useful for the understanding of photodissociation mechanism. The vibrational excitation could be determined²⁶⁻³¹ from the Franck-Condon factor of the initial transition from the ground state to the excited state and the impulsive interaction between the photofragments during the separation period. The vibrational population provides information for the relative roles of these two factors playing in the dissociation dynamics. The bond length of CO in H_2CO is 0.1210 nm,³² which is nearly the same as that for $CO^*(A)$ of 0.12353 nm.³³ This gives the Franck-Condon factor of the initial transition to be the largest at the $v'=0$ level, that is, the $v'=0$ level will have the highest vibrational population and the population decreases with increasing vibrational level. On the other hand, the impulsive interaction will populate the CO fragment to the higher vibrational levels, i.e., the vibrational levels could have a population inversion. The observed population monotonically decreases with increasing vibrational level, indicating that the vibrational population is mainly determined by the initial Franck-Condon transition, and the

impulsive interaction may not be important.

In the UV region, the energy distribution for the process, $\text{H}_2\text{CO} + h\nu (\text{UV}) \rightarrow \text{H}_2(\text{X}, v, J) + \text{CO}(\text{X}, v, J)$, has been studied by Moore and coworkers³⁴⁻³⁷ using laser spectroscopic techniques. It was found that the fragment CO is excited only in $v = 0$ and 1 vibrational states, while the rotational population is highly excited such that the population distribution is highly non-thermal.^{34, 35} The translational energy distribution was also measured by time of flight mass spectroscopy.³⁷ The amount of translational energy was 65% of available energy. It is concluded that the strong repulsive force between the fragments causes high translational energy. The dissociation takes place so fast that the energy can not be randomized among the fragments, that is, the impulsive interaction is not important in the determination of the final vibrational population. Both the excited states involved in the UV and VUV photodissociation seem to have some common characteristics in dissociation dynamics. Theoretical study for the dissociation process of these excited states is of interest.

D. Fluorescence Quantum Yield

The quantum yields for the production of the $\text{CO}(\text{A-X})$ and $\text{HCO}(\text{B-X})$ emissions are shown in Figs. 3a and 3b, respectively. The quantum yield is calculated as the ratio of the fluorescence cross section to the absorption cross section measured at the same monochromator resolution. The quantum yield for the VUV fluorescence increases with decreasing wavelength with a maximum of 1.6% around 116 nm. The UV-visible fluorescence has two

maxima of 0.23% and 0.13% at 116 and 142 nm, respectively. The quantum yields for both the VUV and UV fluorescences decrease substantially at wavelengths below the ionization limit.

As mentioned before, the UV-visible fluorescence includes both the HCO(B-X) system and a fraction of the CO(A-X) system. Since no CO fluorescence appears at wavelengths longer than 140.3 nm, the quantum yield in the 140.3-147.5 nm region is due to the HCO system only. In the 112-140.3 nm region, the UV fluorescence is partly due to the CO(A-X) system whose contribution is about 5% of the VUV quantum yield. For instance, at 116 nm, the quantum yield for the CO fluorescence in the UV region is about 0.08% which is about one-quarter of the total UV fluorescence yield.

As shown in Figs. 3a and 3b, the quantum yield is a smooth function of the excitation wavelength within experimental uncertainty, although both the absorption and fluorescence cross sections show discrete structures. The smooth curves show that the fluorescence yields for the discrete absorption bands are equal to those for the underlying continua. This result implies that the Rydberg states predissociate through the underlying continua. The quantum yields as a function of wavelength can be used to determine the dissociative potential surfaces.³⁸ The photon energy at the maximum quantum yield corresponds to the vertical transition energy of the dissociative potential surface. The vertical energy for the dissociative state that produces the VUV fluorescence is about 10.7 eV. The UV fluorescence is produced by two states with vertical energies of 8.69 and 10.7 eV. The contribution of these two states to the fluorescence

yield is likely to be represented by the dashed-curves shown in Fig. 3b. The VUV and UV fluorescences at excitation wavelengths shorter than 140 nm may be produced through dissociative states that have similar potential surfaces, because the excitation spectra for both fluorescences are very similar. Theoretical understanding of these dissociative states is of interest.

E. Photodissociation Process

The current result is useful for the study of the photodissociation process of H_2CO in the VUV region. For the UV excitation the processes (1) and (2) are the major ones.^{2,12} Similar dissociation processes may occur in the VUV excitation, but the photofragments may be formed in the excited states as well. The photodissociation processes at 123.6 and 147 nm were studied by Glicker and Stief¹⁴, who observed H_2 and CO as the end products. From the end products of deuterated formaldehyde they concluded that the quantum yield for the process (1) or (3) was 50% each.

The threshold for the appearance of the HCO emission is 147.5 ± 0.5 nm (8.41 ± 0.03 eV). If we take the emission to be only due to the $\text{HCO}(\tilde{\text{B}}^2\text{A}' - \tilde{\text{X}}^2\text{A}')$ band¹³ (with an excitation energy of $E(\text{HCO}^*) = 4.83$ eV,^{20,21,39} then the upper limit for the dissociation energy, $D_0(\text{H-HCO}) \leq E_{\text{th}} \pm 3RT/2 - E(\text{HCO}^*)$, is 3.61 ± 0.03 eV (83.4 kcal/mol). Using the thermochemical data⁴⁰: $\Delta H_f^\circ(\text{H}_2\text{CO}) = -25.02$ kcal/mol, $\Delta H_f^\circ(\text{H}) = 51.63$ kcal/mol, the $\Delta H_f^\circ(\text{HCO})$ value determined from the dissociation energy currently obtained is 6.67 kcal/mol. This value is lower than the value of 8.9 ± 1.2 kcal (at 298°K) recommended by Baulch et al.⁴⁰;

however, it is very close to the value of 6.69 kcal/mol obtained by Dyke et al.⁴¹ from photoelectron spectroscopy of HCO radical.

The dissociation energy, $D_0(\text{H-HCO})$, obtained⁴² from the appearance of HCO radical in the UV photolysis of H_2CO is 3.69 - 3.77 eV. Brand and Reed⁴³ suggested that $D_0(\text{H-HCO})$ is less than 3.56 eV as determined from the disappearance of the H_2CO fluorescence in the UV region. Ab initio calculation by Goddard and Schaefer⁴⁴ gave a value of 80.2 kcal/mol (3.48 eV). The upper limit measured in this experiment favors these lower values.

Three electronically excited states of HCO are known.^{32, 45} The lower excited state (\tilde{A}^2A'') was observed only by absorption.^{46, 47} The other two excited states emit, namely, the "Hydrocarbon Flame" A band ($\tilde{B}^2A' - \tilde{X}^2A'$) and the B band ($\tilde{C}^2A'' - \tilde{X}^2A'$).^{20, 21, 35} The potential energy of the \tilde{C}^2A'' state is slightly above the \tilde{B}^2A' state. The excitation energy of the current wavelength region is energetically capable of producing the $\text{HCO}(\tilde{C})$ state whose emission may be that observed in the UV-visible fluorescence. However, Dyne and Style¹³ did not observe the B band emission, suggesting that the contribution of the \tilde{C} state to the observed fluorescence may be small.

The threshold for the production of the $\text{CO}(A-X)$ fluorescence is calculated to be about 7.93 eV (156.3 nm), where the $\text{CO}^*(A)$ energy = 8.028 eV²², $D_0(\text{H}_2-\text{CO}) = -0.095 \text{ eV}$ ⁴⁰ are used in the calculation. The observed threshold at 8.84 eV (140.3 nm) is higher than the calculated value by 0.91 eV. This value may represent the upper limit for the potential barrier between H_2CO^*

and $\text{H}_2+\text{CO}^*(\text{A})$. This value is much lower than the potential barrier for the dissociation of H_2CO into $\text{H}_2+\text{CO}(\text{X})$, which is about 3.5 eV.^{44, 48}

IV. CONCLUDING REMARKS

The photoexcitation process of H_2CO in the 106-180 nm region was studied quantitatively using synchrotron radiation as a light source. The oscillator strengths for the strong Rydberg states were calculated from the absorption cross sections measured. The current oscillator strengths agree very well with the earlier measurements by photoabsorption⁶ and electron scattering.¹⁷ The $\text{CO}(\text{A-X})$ and $\text{HCO}(\text{B-X})$ fluorescence bands were observed from photodissociation of H_2CO whose thresholds are at 140.3 and 147.5 nm, respectively. The vibrational population of the $\text{CO}^*(\text{A})$ state was measured and used to discuss the photodissociation mechanism. The upper limit for the dissociation energy $D_0(\text{H-HCO})$ determined from the UV fluorescence threshold is 3.61 eV.

The fluorescence quantum yield is a smooth function of the excitation wavelength. The HCO fluorescence is produced by two dissociative states whose vertical energies are 8.69 and 10.7 eV. And, the CO fluorescence is produced by a dissociative state of vertical energy 10.7 eV.

Since the photoexcitation of H_2CO in the VUV region leads to dissociation, the photodissociation cross section is essentially equal to the photoabsorption cross section measured. The photoabsorption cross section is thus useful for the calculation of the photodissociation rates of H_2CO by the

interstellar radiation field and the solar radiation field at the earth's upper atmosphere. The calculation of these photodissociation rates will be presented elsewhere.

ACKNOWLEDGEMENT

The authors wish to thank Dr. N. Washida for useful discussion. We thank Dr. E. R. Manzanares, Dr. M. J. Mitchell, Dr. J. B. Nee, and Dr. W. C. Wang in our laboratory for useful discussion and suggestions. The synchrotron radiation facility of the University of Wisconsin is supported by the NSF under Grant No. DMR-80-20164. This material is based on the work supported by the NSF under Grant No. ATM-8412618 and by the NASA under Grant No. NAGW-319.

REFERENCES

1. L. E. Snyder, D. Buhl, B. Zuckerman, and P. Palmer, *Phys. Rev. Lett.* 22, 679 (1969).
2. D. C. Moule and A. D. Walsh, *Chem. Rev.* 75, 67 (1975).
3. W. C. Price, *J. Chem. Phys.* 3, 256 (1935).
4. G. Fleming, M. M. Anderson, A. J. Harrison and L. W. Pickett, *J. Chem. Phys.* 30, 351 (1959).
5. E. P. Gentieu and J. E. Mentall, *Science* 169, 681 (1970).
6. J. E. Mentall, E. P. Gentieu, M. Krauss and D. Neumann, *J. Chem. Phys.*, 55, 5471 (1971).
7. C. R. Lessard and D. C. Moule, *Chem. Phys. Lett.* 29, 603 (1974); *ibid Chem. Phys. Lett.* 47, 300 (1977); *ibid J. Chem. Phys.* 66, 3908 (1977).
8. J. L. Whitten and M. Hackmeyer, *J. Chem. Phys.* 51, 5584 (1970).
9. S. D. Peyerimhoff, R. J. Buenker, W. E. Kramer and H. Hsu, *Chem. Phys. Lett.* 8, 129 (1970); R. J. Buenker and S. D. Peyerimhoff, *J. Chem. Phys.* 53, 1368 (1970).
10. P. W. Langhoff, A. E. Orel, T. N. Rescigno and B. V. McKoy, *J. Chem. Phys.* 69, 4689 (1978).
11. R. D. McQuigg and J. G. Calvert, *J. Am. Chem. Soc.* 91, 1590 (1969).

12. H. Okabe, "Photochemistry of Small Molecules", Wiley, 1978, New York.
13. P. J. Dyne and D. W. G. Style, *Disc. Faraday Soc.* 2, 159 (1947).
14. S. Glicker and L. J. Stief, *J. Chem. Phys.* 54, 2852 (1971).
15. L. C. Lee, *J. Chem. Phys.* 72, 4334 (1980).
16. L. C. Lee and J. A. Guest, *J. Phys. B: At. Mol. Phys.* 14, 3415 (1981).
17. M. J. Weiss, C. E. Kuyatt and S. Mielczarek, *J. Chem. Phys.* 54, 4147 (1971).
18. M. - Th. Praet and J. Delwiche, *Int. J. Mass Spectrom Ion Phys.* 1, 321 (1968).
19. P. M. Guyon, W. A. Chupka, and J. Berkowitz, *J. Chem. Phys.* 64, 1419 (1976).
20. W. M. Vaidya, *Proc. Roy. Soc. A* 147, 513 (1934); *ibid*, *Proc. Phys. Soc.* 64, 428 (1951); *ibid*, *Proc. Roy. Soc. A* 279, 572 (1964).
21. R. N. Dixon, *Trans. Faraday Soc.* 65, 3141 (1969).
22. K. H. Krupenie (Ed), *Natl. Std. Ref. Data Ser.*, Natl. Bur. Std. 5, (1966).
23. R. W. Nicholls, *J. Quant. Spectrosc. Radiat. Transfer* 2, 433 (1962).

24. J. I. Generosa, R. A. Harris, and L. R. Sullo, U. S. Air Force Weapons Laboratory, Technical Report No. AFWL-TR-70-108 (1971).
25. E. Phillips, L. C. Lee, and D. L. Judge, J. Chem. Phys. 66, 3688 (1977).
26. M. J. Berry, Chem. Phys. Lett. 29, 329 (1974).
27. J. P. Simons and P. W. Tasker, Mol. Phys. 26, 1267 (1973).
28. K. E. Holdy, L. C. Klotz, and K. E. Wilson, J. Chem. Phys. 52, 4588 (1970).
29. M. Shapiro and R. D. Levine, Chem. Phys. Lett. 5, 499 (1970).
30. S. Mukamel and J. Jortner, J. Chem. Phys. 60, 4760 (1974).
31. Y. B. Band and K. F. Freed, Chem. Phys. Lett. 28, 328 (1974).
32. G. Herzberg, "Electronic Spectra of Polyatomic Molecules", (Van Nostrand Reinhold, New York, 1966).
33. K. P. Huber and G. Herzberg, "Constants of Diatomic Molecules", (Van Nostrand Reinhold, New York, 1979).
34. P. L. Houston and C. B. Moore, J. Chem. Phys. 65, 757 (1976).
35. D. J. Bamford, S. V. Filseth, M. F. Foltz, J. W. Hepburn and C. B. Moore, J. Chem. Phys. 82, 3032 (1985).

36. D. Debarre, M. Lefebvre, M. Pealat, J.-P. E. Taran, D. J. Bamford and C. B. Moore, *J. Chem. Phys.* 83, 4476 (1985).
37. P. Ho, D. J. Bamford, R. J. Buss, Y. T. Lee and C. B. Moore, *J. Chem. Phys.* 76, 3630 (1982).
38. M. Suto and L. C. Lee, *J. Chem. Phys.* 80, 4824 (1984).
39. M. E. Jacox, *Chem. Phys. Lett.* 56, 43 (1978).
40. D. L. Baulch, R. A. Cox, D. J. Crutzen, R. F. Hampson, Jr., J. A. Kerr, J. Troe and R. T. Watson, *J. Phys. Chem. Ref. Data*, 11, 327 (1982).
41. J. M. Dyke, N. B. H. Jonathan, A. Morris and M. J. Winter, *Mol. Phys.* 39, 629 (1980).
42. J. H. Clark, C. B. Moore and N. S. Nogar, *J. Chem. Phys.* 68, 1264 (1978).
43. J. C. D. Brand and R. I. Reed, *J. Chem. Soc.* 1957, 2386.
44. J. D. Goddard and H. F. Schaefer III, *J. Chem. Phys.* 70, 5117 (1979).
45. K. Tanaka and E. R. Davidson, *J. Chem. Phys.* 70, 2904 (1979); K. Tanaka and K. Takeshita, *Chem. Phys. Lett.* 87, 373 (1982).
46. D. A. Ramsay, *J. Chem. Phys.* 21, 960 (1953); G. Herzberg and D. A. Ramsay, *Proc. R. Soc. London Ser. A* 233, 34 (1956); J. W. C. John, S. H. Priddle and D. S. Ramsay, *Disc. Faraday*

Soc. 35, 90 (1953).

47. R. Vasudev and R. N. Zare, J. Chem. Phys. 76, 5267 (1982).

48. M. Dupuis and W. A. Lester, Jr., B. H. Lengsfeld III, and B. Liu, J. Chem. Phys. 79, 6167 (1983).

FIGURE CAPTIONS

Fig. 1 Absorption and fluorescence cross sections of H_2CO in the 106-180 nm region with a spectral resolution of 0.2 nm. (a) Absorption cross section. The assignments of Rydberg states are adopted from Ref. 6. (b) The cross section* for the production of the VUV fluorescence from photodissociative excitation of H_2CO . The calculated threshold for the $\text{H}_2+\text{CO}^*(\text{A})$ process is indicated. (c) The UV-visible fluorescence cross section. The calculated threshold for the $\text{H}+\text{HCO}^*(\text{B})$ process is indicated.

Fig. 2 The VUV fluorescence spectrum produced from photodissociation of H_2CO at 123.9 nm. The resolution was 1.3 nm and the pressure was 92 mtorr. The wavelength positions of the $\text{CO}(\text{A}, v' - \text{X}, v'')$ vibrational bands are indicated to identify the spectrum.

Fig. 3 The quantum yields for (a) the VUV fluorescence and (b) the UV-visible fluorescence. The ionization potential of H_2CO at 114.2 nm is indicated. The UV-visible fluorescence is produced from two-dissociative states whose contributions are approximated by the dashed curves.

Table I
Integrated absorption cross sections and oscillator strengths

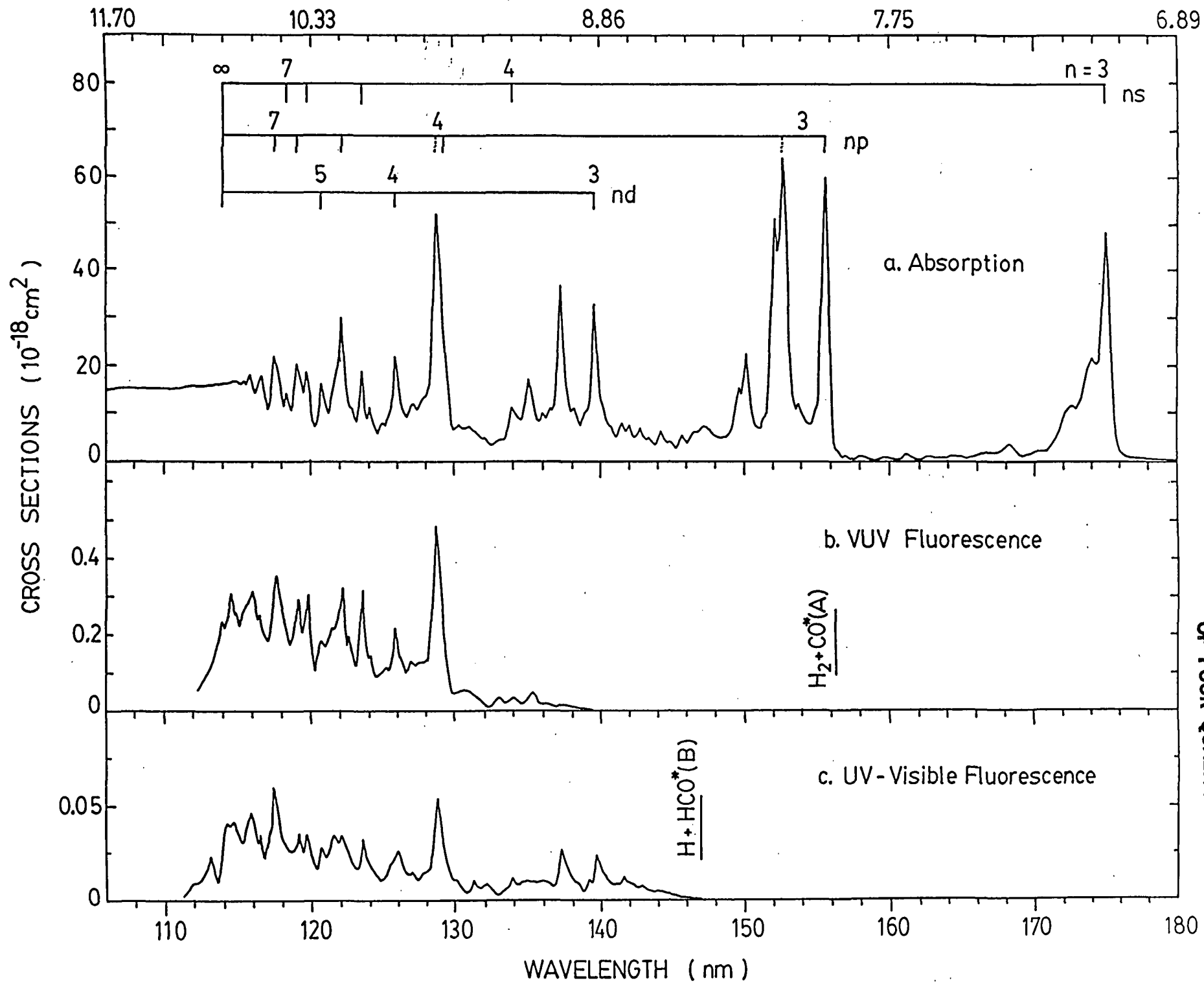
Rydberg State	band peak (nm)	Wavelength region (nm)	$\int \sigma(\lambda) d\lambda$ ($10^{-18} \text{cm}^2\text{-nm}$)	$f^{\text{a)}$	$f^{\text{b)}$	$f^{\text{c)}$
3sa ₁	174.92	165.7-176.7	85.7	0.032	0.038	0.028
3pb ₂	155.55	154.4-156.6	40.6	0.019	0.019	0.017
3pa ₁	152.60	150.9-153.3	73.5	0.036	0.042	0.032
3d(1)	139.55	138.7-141.0	31.0	0.018	0.013	0.015
3d(2)	137.20	136.9-138.6	30.2	0.018	0.016	0.017
4p	128.72	127.4-129.7	55.8	0.038	0.031	0.032
4d	125.85	124.9-126.6	20.6	0.015		
5s	123.55	123.1-124.6	16.0	0.012		
5p	122.18	121.2-123.0	30.2	0.023	0.013	0.022

a) this work

b) from Ref. 6 (the values including the underlying continua).

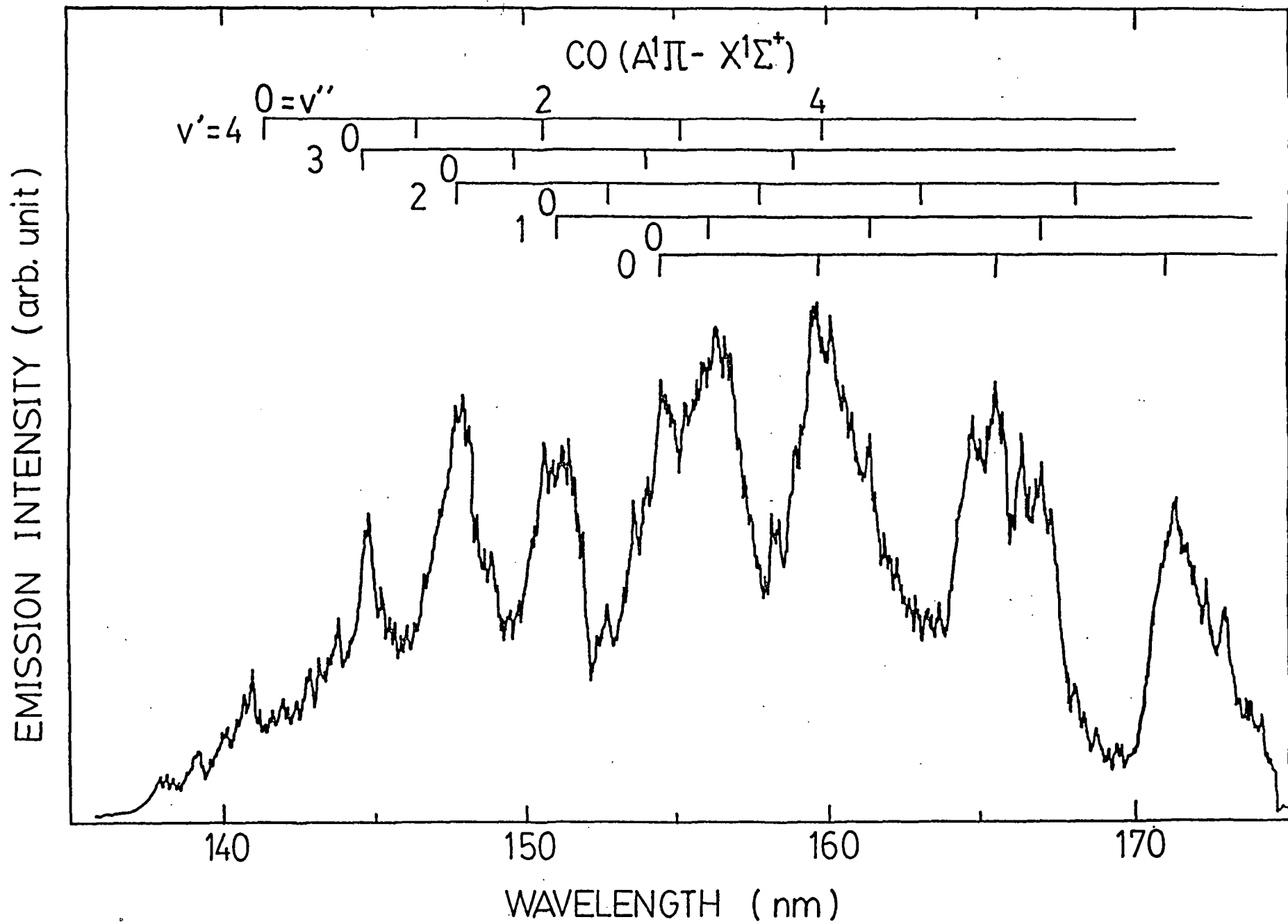
c) from Ref. 17.

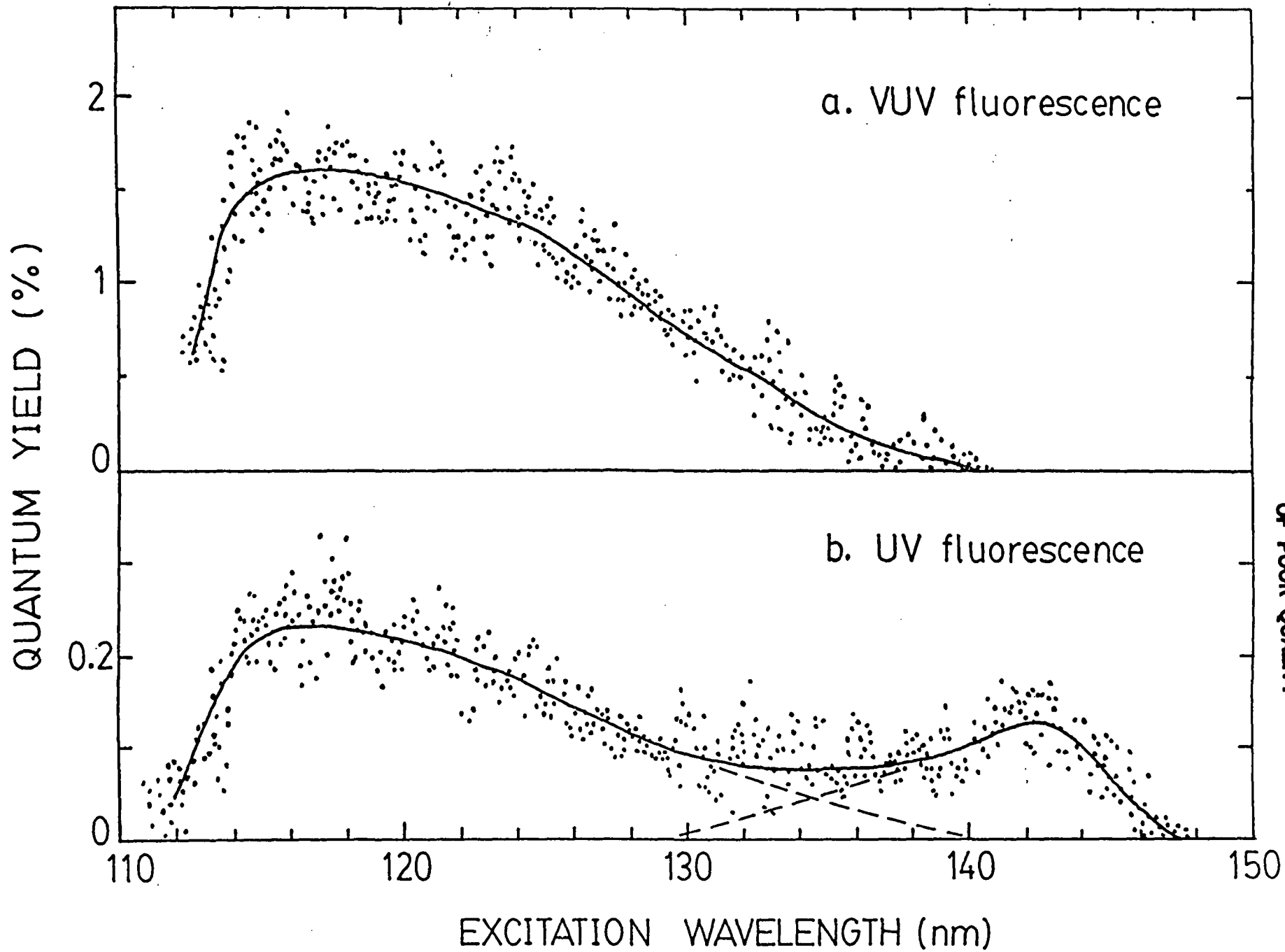
Fig. 1



ORIGINAL PAGE IS
OF POOR QUALITY

Fig. 2





ORIGINAL PAGE IS
OF POOR QUALITY

FIG. 3